Proceedings of the Australian Combustion Symposium
November 6-8, 2013, The University of Western Australia

Mixture Fraction Probability Density Functions in Sparse Spray Flames with Spark Ignition

Andrew P. Wandel *
Computational Engineering and Science Research Centre, School of Mechanical and Electrical Engineering
University of Southern Queensland Qld 4350 Australia

Abstract

Analysis of Direct Numerical Simulation (DNS) data is performed to identify the effects on the mixture fraction probability density function (pdf) of the evaporation region. For the current conditions, the initial droplet field comprises half the initial volume and a spark is used to evaporate and ignite the core of the droplet field. It is found that there is a potentially significant influence on the overall mixture fraction pdf due to the major evaporation region of the droplets. Furthermore, there is a smaller but potentially significant influence on the overall pdf due to the leading edge of the evaporation region. The near-field evaporation field surrounding the droplets can also be significant.

Keywords: Spray combustion, Direct Numerical Simulations, Spark ignition, Mixture fraction, Probability density functions

1. Introduction

Spark ignition for spray combustion is common in gas turbine engines while the automotive industry is adopting it as DISI (Direct-Injection Spark-Ignition) engine technology: an active research area [1–5]. Classic experiments showed that spray flames need more spark energy than equivalent gaseous mixtures to overcome the latent heat of vaporisation, with turbulence impacting negatively on ignition success [6, 7]. The behaviour is sensitive to the droplet size, with fine droplets able to sustain lean flames (when the equivalent gaseous flame cannot) because the gaseous distribution of fuel is more variable, producing local stoichiometric conditions [6].

Conditional Moment Closure (CMC) [8] is a model that advocates argue is well suited to modelling spray flames [8–10]. A derivation of the CMC transport equation for spray combustion [11] has allowed its application [12, 13]. However, there have been few investigations into the mixing of two-phase flows [9], so the β-function probability density function (pdf) is often used to model the mixture fraction pdf, following the single-phase model. Indeed, it was proposed that a model for the gaseous phase in the far-field from the droplets would obey a β-function distribution [10]. In this model, the pdf would be defined so that the limits of mixture fraction would be [0,1] even though the realisable upper limit will almost certainly be much lower. This model deliberately neglects the near-field probability, which occurs at the upper range of realisable mixture fraction.

Zhu *et al*. [14] derived transport equations for a range of joint-pdf definitions, including droplet size distributions and also level-set descriptions to distinguish the probabilities of liquid and gas. However, this work does not seem to have translated into a working model for the mixture fraction pdf. Demoulin & Borghi [15] presented a sketch of how they thought the pdf should look. It contained a high probability at zero mixture fraction, which decays until there is a secondary peak at some finite value of mixture fraction. This bimodal behaviour cannot be modelled by a β-function pdf due to a tail at the largest realisable mixture fractions. They then presented an algebraic model for the pdf.

Direct Numerical Simulations (DNS) provide a tool for characterising the behaviour of spray flames [16] and some DNS studies have presented their mixture fraction pdf with the β-function pdf matching their results well [17, 18]. Other studies have presented the DNS pdf without comparing to a model because the pdf is clearly more complex [19, 20]. This could be due to the near-field region producing high values of mixture fraction that essentially act as an independent distribution [21, 22]. A model for the pdf was proposed [22] based on a suggested model for the near-field distribution [8].

All of those DNS results have been based on analysis of autoigniting spray flames. An analysis [23] of DNS results for spark-ignition spray flames [24] was conducted with the mixture fraction defined to be based on the gas-phase only. The study found that the Favre mixture fraction pdf could be decomposed into a β-function pdf for the lowest values of mixture fraction, with the secondary peak (similar to that described in [15]) modelled by a Gaussian distribution. When the mixture fraction was normalised by the mean mixture fraction, the location of the peak of this secondary Gaussian remained fixed and after the effects of the spark had dissipated, the profile became self-similar. However, it was found that the addition of the tails between the primary β-function pdf and the secondary Gaussian pdf did not account for all of the probability in this region of mixture-fraction space. It was discovered that to model this intermediate region required a tertiary Gaussian pdf. The purpose of this paper is to investigate which regions of physical space produce these three modelled distributions. It will also investigate the need for a fourth distribution at the highest mixture fractions.

* Corresponding author:
Phone: (+61) 7 4631 2230
Email: andrew.wandel@usq.edu.au

2. Background

The three-dimensional compressible DNS code SENGA [25] was used with periodic boundary conditions in the y- and z-dimensions and partially non-reflecting boundary conditions [26] for the x-direction. The fuel was initially solely contained in the liquid phase, with the droplets uniformly distributed in the central portion of the domain, leaving pure air between the boundaries in the x-direction and the droplet field. This is because the boundary conditions for droplets entering the domain are unclear. The droplet transport equations accounted for the relaxation to the gaseous phase values of velocity and temperature in addition to the effect of evaporation on droplet temperature and diameter [27, 28]. The gas phase was coupled via droplet source terms in the continuity, momentum, energy and species transport equations. A single-step irreversible chemical mechanism was used [29], while the spark was modelled by the deposition of energy for a fixed duration t_{sp}, with the spatial distribution of the power a Gaussian distribution as a function of radius from the centre of the domain. Full details on the implementation for the case under consideration can be found elsewhere [24, 30]. Of primary interest here is the definition of mixture fraction used, which is based solely on the gaseous phase:

$$Z = \frac{Y_F - Y_O/s + Y_{O,i}/s}{Y_{F,i} + Y_{O,i}/s} \qquad (1)$$

where Y is the mass fraction of either Fuel or Oxidiser, with i representing the inlet stream value, and s is the stoichiometric mass of oxidiser per unit mass of fuel. For the fuel considered (n-heptane), the values in this case are $Y_{F,i}$ = 1.0, $Y_{O,i}$ = 0.233 and s = 3.52, while the stoichiometric mixture fraction is 0.062.

3. Results

The case of interest is what is defined as the "base case" in Ref. [24]: a case where the spark evaporated sufficient fuel to create an ignitable mixture with the flame propagating successfully for the duration of the simulation. Figure shows the mixture fraction Favre pdf for the instant at $0.5t_{sp}$; at this time the mean mixture fraction was 0.0140, so essentially no mixture was above the stoichiometric value. Note that the pdf is determined for the entire computational domain and is based on the mixture fraction values occurring at each node in the DNS grid. The modelled pdf is the summation of the component pdfs, where each component pdf is scaled so that its integral is no longer unity. When determining the modelled pdf for this instant, it was observed that only using the primary β-function pdf with the secondary and tertiary Gaussian pdfs grossly under-predicted the pdf beyond the peak at $Z \approx 1.8\langle Z\rangle$. Another phenomenon is occurring at these high mixture fraction values, which requires modelling by a Gaussian distribution. Once this is done, the modelled pdf predicts the actual pdf well.

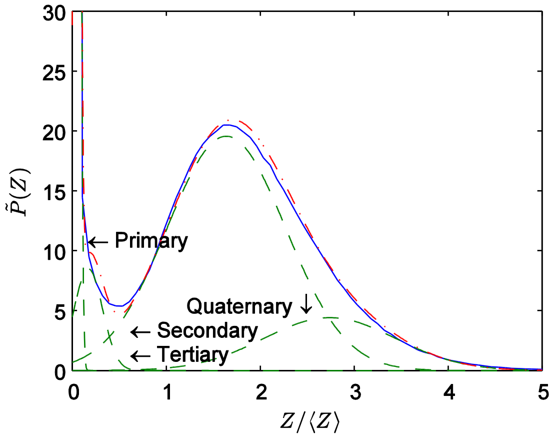

Figure 1: Mixture fraction Favre pdfs at $t = 0.5t_{sp}$, when $\langle Z\rangle = 0.0140$. DNS [24], —; model, – ·; primary β-function pdf, secondary, tertiary and quaternary Gaussian pdfs, – –.

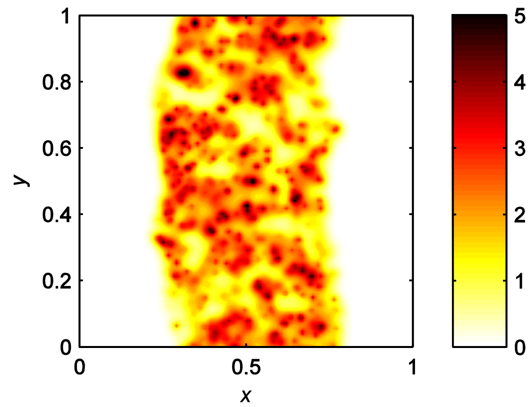

Figure 2: Slice of normalised mixture fraction $Z/\langle Z\rangle$ at time corresponding to Fig. 1 for $z = 0.5$.

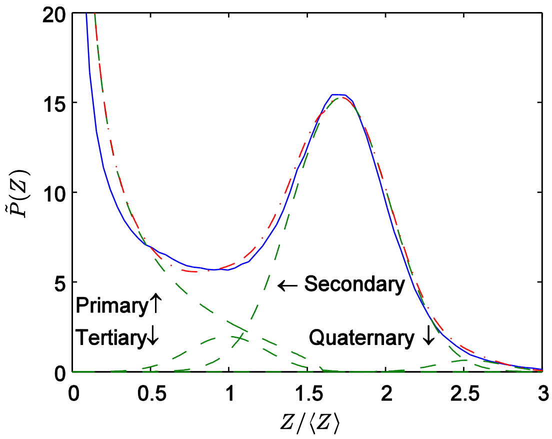

Figure 3: Mixture fraction Favre pdfs at $t = 4t_{sp}$, when $\langle Z\rangle = 0.0387$. As per Fig. 1.

An explanation for the behaviour is shown in Fig. 2: a sample of the mixture fraction field. The quaternary pdf is due to the field immediately surrounding the droplets, which occupies a substantial amount of space (has high probability) because of the evaporation due to the ambient temperature (ignition is yet to occur [24, 30]). The secondary pdf is created as the gaseous fuel mixes with the surroundings. The primary β-function pdf dominates due to insufficient spread of the fuel.

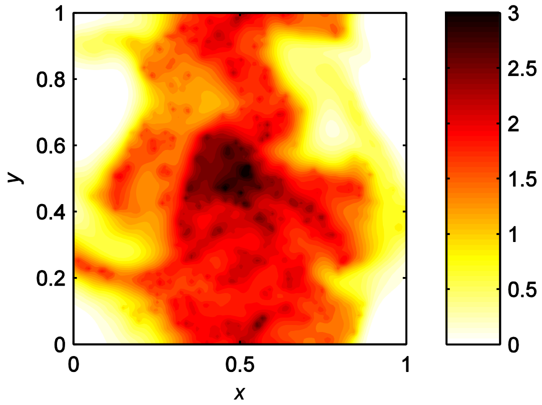

Figure 4: Slice of normalised mixture fraction $Z/\langle Z\rangle$ at time corresponding to Fig. 3 for $z = 0.25$.

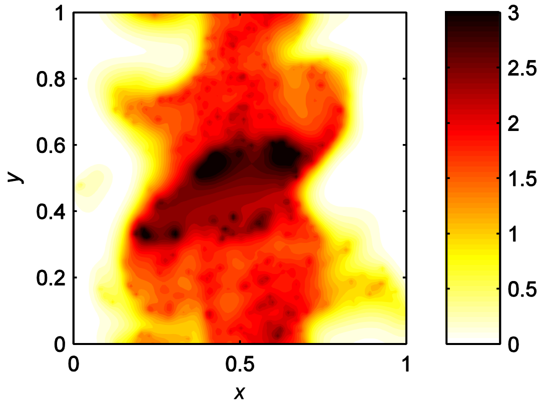

Figure 5: As per Fig. 4 for $z = 0.5$.

Note that the tertiary pdf is necessary to model other behaviour which is not captured by the primary and secondary pdfs. An explanation for the cause of the tertiary pdf is more easily observed at the later time $4t_{sp}$, when the effects of the spark have dissipated. Figure 3 shows that while the peak of the secondary pdf has remained at approximately the same normalised mixture fraction value, its relative width has diminished (the greatly increased value of $\langle Z\rangle$ means the absolute width has increased). This has caused the tertiary pdf to move a large distance to the right. Looking at the representative samples throughout the domain of the distribution of (normalised) mixture fraction (Figs. 4–7), the value of 1 is observed on the edges of the interface between the pure air and the droplet region. While its effect may be small compared to the primary and secondary pdfs, it has a significant influence in the vicinity of the mean mixture fraction at the later time. Its creation is due to the large gradients of mixture fraction at the leading edge of the evaporation region. This phenomenon can be seen in the DNS because it spatially resolves the leading edges.

The quaternary pdf is only responsible for a smaller amount of the overall distribution and this is restricted to the region surrounding the spark centre (located at [0.5,0.5,0.5]): Figs. 4 and 5. This region corresponds to the only part of the domain where combustion has occurred (Figs. 8 and 9), and this has accelerated the droplet evaporation.

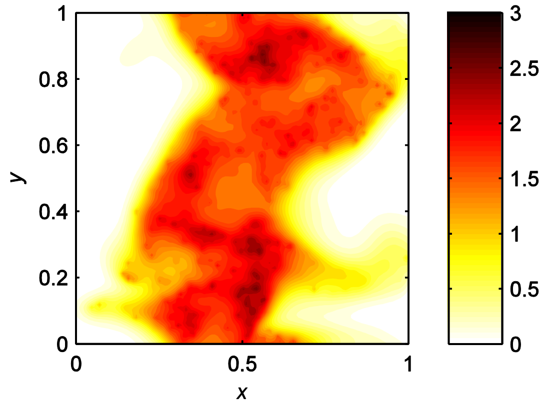

Figure 6: As per Fig. 4 for $z = 0.75$.

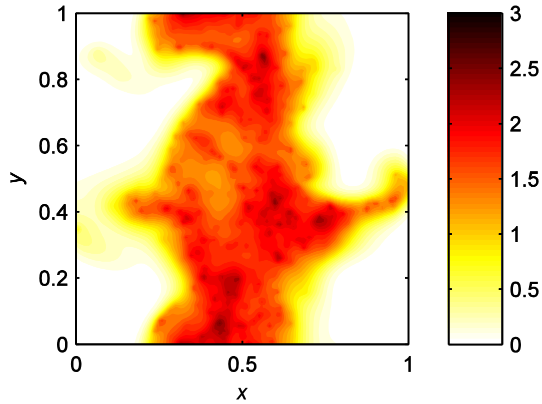

Figure 7: As per Fig. 4 for $z = 1$.

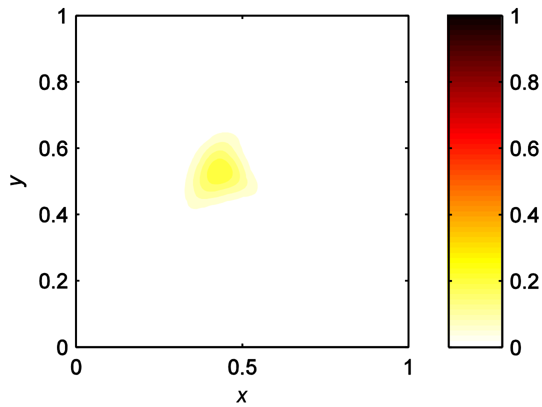

Figure 8: Slice of non-dimensional temperature for same conditions as Fig. 4.

The primary β-function pdf represents the pure air, so its strength would be greater for a substantially wider computational domain (the initial droplet region was half the volume). Its significant influence above the mean mixture fraction at later times is probably due to the large regions near the boundaries of the domain with low gradients of mixture fraction ahead of the mean mixture fraction (e.g. Fig. 6 for $y \approx 0.2$ at the highest x).

4. Conclusions

This study has demonstrated that while the mixture fraction pdf is dominated by a β-function distribution, there can be a significant influence of the droplet evaporation region on the shape of the pdf at values of mixture fraction greater than the mean. Furthermore, the leading edge of the evaporation region produces a smaller, yet potentially significant, influence on the overall pdf. This effect could be important when considering the modelling of the edges of spray jets. Finally, there is a localised effect due to the evaporation of the droplets. This effect was greatest in the current case before the spark had ignited the mixture, when the entire droplet field was evaporating due to ambient conditions. Once the spark ignited the mixture in the centre of the domain, the greatly increased temperature accelerated the droplet evaporation and caused the quaternary distribution to have a relatively minor influence overall due to the relatively small spark size. It can therefore be hypothesised that autoignition cases will be dominated more by this effect.

Nonetheless, if the overall volume of the domain under consideration contains substantially more pure oxidiser than droplet-laden oxidiser, it is likely that the secondary peak will have an insignificant mode compared to the β-function pdf component for the corresponding range of mixture fraction values. This potentially validates the assumptions that were made in using a β-function pdf to model the mixture fraction pdf [10]. Firstly, neglecting the near-field (which is not fully resolved in the current results) due to its low probability: the percentage of volume that could be considered to be occupied by the droplets here is very small. Secondly, applying the limits used in defining the β-function pdf to be the full range of mixture fraction, rather than a subset which accounts for the low realisable range. Stretching the tail in this manner would likely assign a higher probability to the mixture fractions influenced by the secondary pdf and thereby account for some of the effects of it and the quaternary pdf, while removing the need for the tertiary pdf.

Future work will investigate the extent to which the current results are sensitive to variables such as droplet number density, initial diameter and flame success.

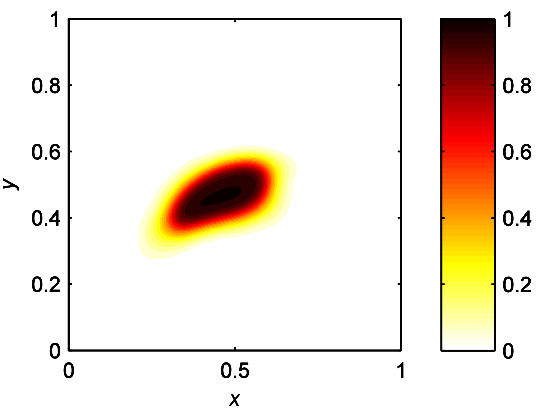

Figure 9: Temperature for same conditions as Fig. 5.

5. References

[1] R. Anderson, A New Direct Injection Spark Ignition (DISI) Combustion System for Low Emissions, Technical Report P0201, FISITA, 1996.

[2] P. G. Aleiferis, J. Serras-Pereira, Z. van Romunde, J. Caine, M. Wirth, Combust. Flame 157 (2010) 735–756.

[3] H. Kwon, H. Choi, J. Kim, K. Min, Combust. Theory Modelling 16 (2012) 1089–1108.

[4] M. Sjöberg, D. L. Reuss, Proc. Combust. Inst. 34 (2013) 2933–2940.

[5] D. Goryntsev, A. Sadiki, J. Janicka, Proc. Combust. Inst. 34 (2013) 2969–2976.

[6] S. K. Aggarwal, Progr. Energy Combust. Sci. 24 (1998) 565–600.

[7] A. H. Lefebvre, Gas Turbine Combustion, Taylor and Francis, 1999.

[8] A. Y. Klimenko, R. W. Bilger, Progr. Energy Combust. Sci. 25 (1999) 595–687.

[9] E. Mastorakos, Progr. Energy Combust. Sci. 35 (2009) 57–97.

[10] R. W. Bilger, Combust. Flame 158 (2011) 191–202.

[11] M. Mortensen, R. W. Bilger, Combust. Flame 156 (2009) 62–72.

[12] S. Ukai, A. Kronenburg, O. T. Stein, Proc. Combust. Inst. 34 (2013) 1643–1650.

[13] M. Bolla, Y. M. Wright, K. Boulouchos, G. Borghesi, E. Mastorakos, Combust. Sci. Tech. 185 (2013) 766–793.

[14] M. Zhu, K. N. C. Bray, O. Rumberg, B. Rogg, Combust. Flame, 122 (2000) 327–338.

[15] F. X. Demoulin, R. Borghi, Combust. Sci. Tech. 158 (2000) 249–271.

[16] P. Jenny, D. Roekaerts, N. Beishuizen, Progr. Energy Combust. Sci. 38 (2012) 846–887.

[17] S. Sreedhara, K. Y. Huh, Proc. Combust. Inst. 31 (2007) 2335–2342.

[18] H. Wang, K. Luo, J. Fan, Energy 46 (2012) 606–617.

[19] J. Seo, K. Y. Huh, Proc. Combust. Inst. 33 (2011) 2127–2134.

[20] J. Seo, K. Y. Huh, Proc. Combust. Inst. 34 (2013) 1687–1695.

[21] P. Schroll, A. P. Wandel, R. S. Cant, E. Mastorakos, Proc. Combust. Inst. 32 (2009) 2275–2282.

[22] M. R. G. Zoby, S. Navarro–Martinez, A. Kronenburg, A. J. Marquis, Int. J. Heat Fluid Flow 32 (2011) 499–509.

[23] J. Clarke, A. P. Wandel, E. Mastorakos, Analysis of Data to Develop Models for Spray Combustion, in: Proceedings of the Southern Region Engineering Conference, 11–12 November 2010, 2010, p. SREC2010-F2-1.

[24] A. P. Wandel, N. Chakraborty, E. Mastorakos, Proc. Combust. Inst. 32 (2009) 2283–2290.

[25] K. W. Jenkins, R. S. Cant, in: Proceedings of the Second AFOSR Conference on DNS and LES, Kluwer Academic, 1999, pp. 192–202.

[26] T. J. Poinsot, S. K. Lele, J. Comput. Phys. 101 (1992) 104–129.

[27] J. Réveillon, L. Vervisch, Combust. Flame 121 (2000) 75–90.

[28] J. Réveillon, L. Vervisch, J. Fluid Mech. 537 (2005) 317–347.

[29] N. Chakraborty, E. Mastorakos, R. S. Cant, Combust. Sci. Tech. 179 (2007) 293–317.

[30] A. P. Wandel, Proc. Combust. Inst. 34 (2013) 1625–1632.